



OPEN

A new DNA aptamer which binds to SARS-CoV-2 spike protein and reduces pro-inflammatory response

Woong Kim¹, Eun Su Song², Song Ha Lee³, Seung Ho Yang⁴, Junhyung Cho⁵ & Seok-Jun Kim^{1,6,7}✉

COVID-19 caused by SARS-CoV-2 spread rapidly around the world, endangering the health of people globally. The SARS-CoV-2 spike protein initiates entry into target cells by binding to human angiotensin-converting enzyme 2 (ACE2). In this study, we developed DNA aptamers that specifically bind to the SARS-CoV-2 spike protein, thereby inhibiting its binding to ACE2. DNA aptamers are small nucleic acid fragments with random structures that selectively bind to various target molecules. We identified nine aptamers targeting the SARS-CoV-2 spike protein using the systematic evolution of ligands by exponential enrichment (SELEX) method and selected three optimal aptamers by comparing their binding affinities. Additionally, we confirmed that the DNA aptamers suppressed pro-inflammatory cytokines induced by the SARS-CoV-2 spike protein in ACE2-overexpressing HEK293 cells. Overall, the DNA aptamer developed in this study has the potential to bind to the SARS-CoV-2 spike protein and inhibit or block its interaction with ACE2. Thus, our DNA aptamers can be used as new biological tools for the prevention and diagnosis of SARS-CoV-2 infection.

Keywords Aptamer, SARS-CoV-2, ACE2, Prevention, Diagnostic

Severe acute respiratory syndrome coronavirus-2 (SARS-CoV-2), responsible for the coronavirus disease (COVID-19) pandemic in 2019, has spread rapidly worldwide and has caused respiratory illnesses in large populations^{1,2}. Viral infections can cause various adverse effects, including respiratory complications. Increased local inflammation induces excessive cytokine production or a cytokine storm, which leads to a systemic inflammatory response syndrome³⁻⁵. SARS-CoV-2 is a single-stranded RNA virus comprising a spike, membrane, envelope, and nucleocapsid³. The extracellular domain spike protein plays a key role in receptor recognition and cell membrane fusion, and contains a receptor-binding domain (RBD) that binds to the angiotensin-converting enzyme 2 (ACE2) receptor in humans. The RBD of the S1 subunit of SARS-CoV-2 binds ACE2 and initiates its entry into target cells⁶.

The characteristics of SARS-CoV-2 are closely associated with its detection, prevention, and treatment. Early detection of SARS-CoV-2 is essential for its rapid isolation and contact tracing to reduce the risk of transmission⁷. Clinical detection, a common detection method for SARS-CoV-2 based on clinical symptoms and contact history with other potentially infected individuals, resulting in unreliable results in asymptomatic and inaccurate contact histories. Therefore, various molecular-technology-based diagnostic tests for SARS-CoV-2 have been developed. Two representative detection methods are viral nucleic acid detection methods such as reverse transcription polymerase chain reaction (RT-PCR) and quantitative real-time PCR (qPCR)^{8,9}, and an immunoassay using SARS-CoV-2-specific IgM/IgG¹⁰⁻¹². mRNA vaccines Pfizer–BioNTech (BNT162b2)¹³ and Moderna COVID-19

¹Institute of Well-Aging Medicare & Chosun University LAMP Center, Chosun University, Gwangju 61452, Republic of Korea. ²Corporate Research Institute, UNICOMPANY, Gwangju 61008, Republic of Korea. ³Department of Business Management, UNICOMPANY, Gwangju 61008, Republic of Korea. ⁴Department of Planning Management, UNICOMPANY, Gwangju 61008, Republic of Korea. ⁵Division of Emerging Viral Diseases and Vector Research, Centre for Infectious Diseases Research, Korea National Institute of Health, Korea Centres for Disease Control and Prevention Agency, Cheongju 28159, Republic of Korea. ⁶Department of Integrative Biological Sciences & BK21 FOUR Educational Research Group for Age-Associated Disorder Control Technology, Chosun University, Gwangju 61452, Republic of Korea. ⁷Department of Biomedical Science, Chosun University, Gwangju 61452, Republic of Korea. ✉email: heaven1472@chosun.ac.kr

(mRNA-1273)¹⁴ are currently being used to prevent the spread of SARS-CoV-2. mRNA vaccines show high efficacy in preventing SARS-CoV-2 infection, but have disadvantages such as the need for a booster shot, difficulty in storage and transport, and unknown side effects. Treatment strategies for SARS-CoV-2 infection are being researched, including antiviral drugs (*remdesivir*, *favilavir*), anti-HIV drugs (*lopinavir*, *ritonavir*), and ACE2 inhibitors (*APN01*)^{15,16}. Despite research efforts to treat SARS-CoV-2 infections, an effective treatment strategy has not yet been developed. Various strategies have been proposed for the prevention, detection, and treatment of SARS-CoV-2 infection, and on-going research is being based on the direct spike protein–ACE2 interaction with a focus on development of biomolecules, such as antibodies^{17,18} and aptamers^{19–21}, that block this binding, preventing entry of the virus.

Aptamers are small nucleic acid fragments (DNA or RNA) with stable 3D structures that can bind to various target molecules with high affinity and selectivity²². Aptamers have several advantages and are used in various fields. In particular, compared to antibodies, they have advantages such as cost-effectiveness, smaller size, and lower immunogenicity²³. Systematic evolution of ligands by exponential enrichment (SELEX) refers to the process of selecting an aptamer that binds to a specific target through an iterative selection process from a random sequence pool²⁴. These aptamers are distinct from other nucleic acid-based therapies because they often have no direct effect on the steps prior to the protein function²⁵. No significant differences exist in the affinities of DNA and RNA aptamers; however, DNA aptamers are more stable and therefore greatly applicable in many fields²⁶.

In this study, we identified aptamers targeting SARS-CoV-2 spike proteins using the SELEX method. Nine aptamer candidates were screened using SELEX. Among these, three optimal aptamers were selected based on their binding affinities, and their superiority was confirmed by comparison with previously developed aptamers. In addition, the secondary structures of the three selected aptamers were predicted to confirm their structural characteristics. Finally, the selected aptamers were tested with the SARS-CoV-2 spike protein in ACE2-over-expressing Human embryonic kidney 293 (HEK293) cells, and the pro-inflammatory response was examined.

Materials and methods

SELEX procedures

We performed an aptamer selection procedure for the SARS-CoV-2 spike protein using our modified SELEX method. The single-stranded DNA (ssDNA) library was constructed from two regions with PCR primers on either side, and a region with 40 random sequences in the middle (5'-ATG CGA ATT CAT CAG TGC CAG TCA T—N40—GAT TAG CAT AGA TGA GGA TCC ATG C-3'). First, the ssDNA library was annealed at 95 °C and immediately cooled on ice for 10 min. The DNA aptamer that was non-specifically bound to the nickel–nitrilotriacetic acid (Ni–NTA) magnetic nanobeads was removed through a pre-cleaning step. To select DNA aptamers that specifically bind to the recombinant human coronavirus SARS-CoV-2 spike glycoprotein S1 (His tag; ab273067; Abcam, UK), the interaction between pre-cleaned DNA aptamers and spike proteins was mediated at 4 °C on a rotator for 30 min. The spike protein became bound to the DNA aptamer that had specifically bound to the Ni–NTA magnetic nanobeads (Bioneer, Daejeon, Korea) in a binding buffer containing 50 mM sodium phosphate, 500 mM NaCl, and 10 mM imidazole, pH 8.0. The aptamer–protein–nanobead conjugate was now separated using a magnet, and the supernatant was removed. The recovered beads were then washed five times with binding buffer. After washing, the DNA aptamer–protein component was released from the nanobeads in the conjugate using an elution buffer containing 50 mM sodium phosphate, 500 mM NaCl, and 500 mM imidazole, pH 8.0. The recovered DNA aptamer–protein was added to the PCR mixture TOPsimple™ PCR DyeMIX-nTaq, which included nTaq (0.2 unit/μL), nTaq buffer with 3 mM MgCl₂, dNTP mixture (0.4 mM each), stabilizer, and dyes (Xylene cyanol and Orange G) from Enzynomics (Daejeon, Korea). The mixture was amplified using forward (5'-ATG CGA ATT CAT CAG TGC CAG TCA T-3') and reverse (5'-GAT TAG CAT AGA TGA GGA TCC ATG C-3') primers to amplify the target-bound sequences. PCR steps of denaturation, annealing, and extension were cycled 25 times to amplify the target DNA. The resulting PCR product, approximately 100 bp in size, was separated by agarose gel electrophoresis and purified using an Expin Combo GP Mini Kit from GeneAll (Seoul, Korea). After elution of the double-stranded DNA, it was incubated with 5 U of lambda exonuclease from Enzynomics (Daejeon, Korea) in a total reaction volume of 20 μL at 37 °C. The reaction was terminated after 30 min by incubating at 75 °C for 10 min. The resulting ssDNA product was used in the next round of the selection process, and this process was repeated four times, with the amount of protein (1, 0.5, 0.25, 0.1 μg) decreasing at each step.

Cloning and sequencing aptamers

The pGEM®-T Easy Vector System (Promega, CA, USA) was used to clone the various aptamers selected through SELEX. The pGEM®-T Easy Vector was provided in linear form with a single 3'-T overhang for TA cloning. The selected aptamers were amplified with the addition of adenine (A) at the 3'-termini using Ex Taq™ (Takara, Shiga, Japan), and the PCR products were used for cloning. The PCR products and pGEM®-T Easy Vector were ligated at 4 °C overnight using T4 DNA ligase. Next, aptamers + pGEM®-T Easy Vector constructs were transformed into HIT Competent Cells™-DH5α (RBC, Toronto, Canada), and the resulting colonies were screened by ampicillin. The plasmid DNA was purified using the FavorPrep™ Plasmid Extraction Mini Kit (FAVORGEN, Taipei City, Taiwan). Plasmid DNA was sequenced by Sanger sequencing (Macrogen, Seoul, Korea).

Comparison of binding affinity

To measure the binding efficiency of aptamers, 2 μM of candidate aptamers were mixed with 0.5 μg/mL of the spike protein, followed by incubation at 4 °C for 30 min. The spike protein bound to the DNA aptamers was incubated with Ni–NTA magnetic nanobeads and the conjugate was separated using a magnet, with the supernatant removed. The recovered beads were then washed five times with a binding buffer, and the aptamers were

released from the nanobeads using an elution buffer. The candidate aptamers were detected using TOPreal™ SYBR Green qPCR PreMix (Enzynomics, Daejeon, Korea) to obtain the standard curve for real-time PCR analysis. Cycle threshold (Ct) values of the candidate aptamers were compared using a Rotor-Gene 3000 real-time PCR system (Corbett Research, Australia). All analyses were performed in triplicate and Ct values were calculated from the average of each measurement.

Secondary structure prediction

The RNAfold web server (<http://rna.tbi.univie.ac.at>)²⁷ was used to predict the secondary structures of DNA aptamers. RNAfold can be used to predict the secondary structures of single-stranded RNA or DNA sequences. It uses a partition function for sequences of up to 7,500 nt and a minimum free energy algorithm for sequences of up to 10,000 nt to predict the secondary structures.

Cell culture and transfections

HEK293 cells were purchased from the Korea Cell Line Bank (KCLB, Seoul, Korea). The cell lines were cultured in a Dulbecco's Modified Eagle Medium (DMEM) (WELGENE Inc., Gyeongsan-si, Korea) supplemented with 10% fetal bovine serum (Corning Costar, NY, USA) and 1% penicillin/streptomycin (Gibco, NY, USA) at 37 °C in a 5% CO₂ atmosphere. ACE2 overexpression in HEK293 cells was induced using pcDNA3.1-ACE2. The human ACE2 plasmid was obtained from Addgene (#154962)²⁸. Transfections were carried out using Lipofectamine 2000 reagent (Invitrogen, Carlsbad, CA, USA) according to the manufacturer's instructions.

RNA isolation, cDNA synthesis, and qPCR

Total RNA was isolated from HEK293 cells using RNAiso Plus reagent (Takara, Shiga, Japan), and cDNA was synthesized using ReverTra Ace™ qPCR RT Master Mix (TOYOBO, Osaka, Japan) according to the manufacturer's protocols. The expression level of IL-1β, IL-6, and TNF-α was measured in Rotor-Gene 3000 real-time PCR system (Corbett Research, Australia) using TOPreal™ SYBR Green qPCR PreMIX (Enzynomics, Daejeon, Korea).

Western blotting

HEK293 cells were lysed using RIPA buffer supplemented with a protease inhibitor cocktail (GenDEPOT, TX, USA). The prepared proteins were separated by sodium dodecyl sulfate–polyacrylamide gel electrophoresis and electrotransferred to PVDF membrane (Millipore, MA, USA). The blocking step was carried out using 5% skim milk and washed three times with washing buffer (1X PBS and 0.05% Tween 20). After washing, the membrane was incubated over-night at 4 °C with ACE2 (sc-390851, SCBT, CA, USA) and GAPDH antibodies (AP0066, Bioworld Technology, MN, USA), and secondary antibodies were incubated for 2 h at room temperature. Finally, protein expression levels were detected using ECL solution (Bio-Rad, Hercules, CA, USA).

ELISA

An ELISA test was used to analyze culture medium cytokine (IL-1β, IL-6, and TNF-α) levels in HEK293 cells with SARS-CoV-2 spike glycoprotein S1 and aptamer. HEK293 cells overexpressing ACE2 were treated with SARS-CoV-2 spike glycoprotein S1 and aptamers for 24 h. After incubation, the culture medium was collected and immediately frozen for further analysis. The concentrations of IL-1β, IL-6, and TNF-α in culture medium were measured using ELISA kit (Invitrogen, MA, USA) in accordance with the manufacturer's protocol.

Statistical analysis

P-values < 0.05 were considered to be statistically significant. Statistical analyses were performed using GraphPad Prism version 8. Statistical differences between groups were analyzed using Student's *t*-test. (*, **, ***, and ns indicate *P* < 0.1, *P* < 0.01, *P* < 0.001, and not significant, respectively).

Results

Selection and identification of DNA aptamers against the SARS-CoV-2 spike protein

SARS-CoV-2 spike protein-specific aptamers were selected using the SELEX method²⁹. A modified SELEX method was used to identify single-stranded DNA aptamers that could bind to the SARS-CoV-2 spike protein and inhibit its binding to the ACE2 receptor. The selection process of specific ssDNA aptamers for the SARS-CoV-2 spike protein leveraged the properties of the Ni-NTA nanobeads. Initially, the ssDNA aptamer was bound to the His-tagged SARS-CoV-2 spike protein, and this binding complex was subjected to a selection process using Ni-NTA nanobeads capable of binding to the His-tagged protein. The selected aptamers were amplified by PCR, and the SELEX process was repeated four times to enhance the binding affinity of the aptamers (Fig. 1). After each selection round, the DNA aptamers were amplified via PCR and subsequently cloned into chemically competent *E. coli* using the pGEM®-T Easy Vector Systems. The sequences of the nine individual aptamer clones were determined (Table 1). These nine new sequences were previously unexplored; therefore, subsequent experiments were performed using these sequences.

Comparison of binding affinity between candidate DNA aptamers

To evaluate the binding affinity of the SARS-CoV-2 spike protein to the candidate DNA aptamers, qPCR analysis was conducted. When the binding of the target protein and DNA aptamer was induced under the same conditions, the aptamer with higher affinity showed more binding, and these aptamers were harvested again and quantified by qPCR. Put differently, the lower the Ct value (high concentration of DNA aptamer), the higher the binding affinity of the DNA aptamer to its target^{30–33}. Therefore, by monitoring the change in Ct values using

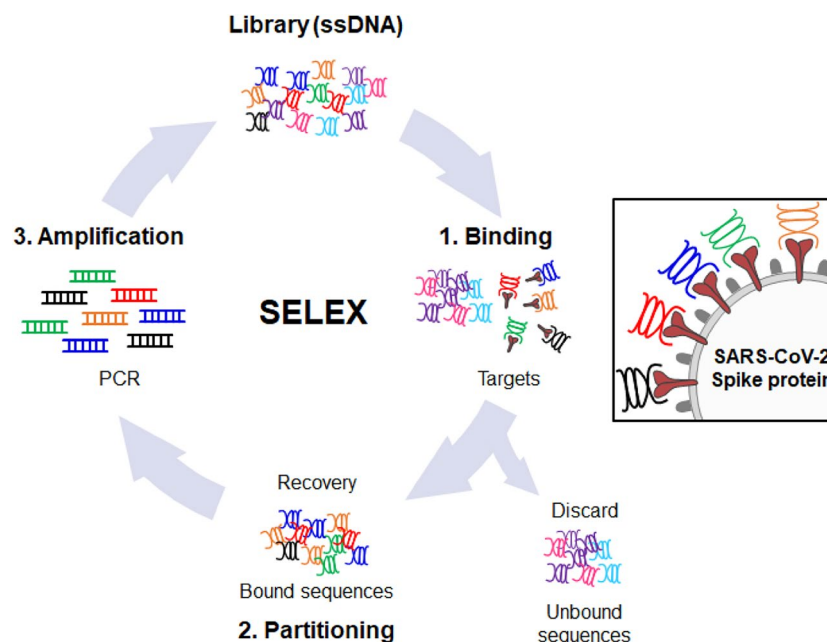


Figure 1. Schematic description of SELEX in the selection against the SARS-CoV-2 spike protein. Initially, a pre-clearing step was performed by incubating single-stranded DNA (ssDNA) libraries with Ni-NTA nanobeads to remove Ni-NTA binding ssDNA. The remaining unbound ssDNA was then mixed with SARS-CoV-2 spike proteins for the selection process. The binders, which specifically bound to the spike proteins, were subsequently eluted and amplified using PCR. This process was repeated four times to enhance the binding affinity of the aptamers. Finally, the DNA aptamer with improved binding affinity was cloned and its sequence was determined through sequencing.

No	Name	5'-Oligo Seq-3'
1	SC2_R4_1	ATG CGA ATT CAT CAG TGC CAG TCA TTT CCG GTG GTC TTC GCA TAC GGC TTG ATT TGA TGC GGA TTA GCA TAG ATG AGG ATC CAT GC
2	SC2_R4_3	GCA TGG ATC CTC ATC TAT GCT AAT CCG TAG ACG CGT GAG GCA GCC GTA TGC GAA TCG GCA CTC CCA ACG ATG ACT GGC ACT GAT GAA TTC GCA T
3	SC2_R4_4	GCA TGG ATC CTC ATC TAT GCT AAT CGT TGA CAC CAG CAT ATG CGA ATC GGA GAT AAG AGG ATG ACT GGC ACT GAT GAA TTC GCA T
4	SC2_R4_5	ATG CGA ATT CAT CAG TGC CAG TCA TTT GCG GGT GTG TCG CTC GTC TTC GCA TAG GTG GCG CGT TGG ATT AGC ATA GAT GAG GAT CCA TGC
5	SC2_R4_8	GCA TGG ATC CTC ATC TAT GCT AAT CAC GAC CCA TAC GTC GTG GCT AGT ATG CGA AGA CCC CAA GAT GAC TGG CAC TGA TGA ATT CGC AT
6	SC2_R4_10	GCA TGG ATC CTC ATC TAT GCT AAT CCC AAT GAC GCG GAC GTA TGC GAA GGC GGA TCA AAT AGA TGA CTG GCA CTG ATG AAT TCG CAT
7	SC2_R4_13	ATG CGA ATT CAA TCA GTG CCA GTC ATT TGC GGG TGT GTC GCT CGT CTT CGC ATA GGT GGC GCG TTG GAT TAG CAT AGA TGA GGA TCC ATG C
8	SC2_R4_14	ATG CGA ATT CAT CAG TGC CAG TCA TTC TCG GGG TGC GTA TTC GCA TAA GCC CCA TCT TCA GAC CAG ATT AGC ATA GAT GAG GAT CCA TGC
9	SC2_R4_16	ATG CGA ATT CAT CAG TGC CAG TCA TGC GTT TCC GGT CTT CGC ATA CGT TCT CTG TCC TGG CTT GAT TAG CAT AGA TGA GGA TCC ATG C

Table 1. List of DNA aptamers with insert sequences.

qPCR, the binding affinity of the protein target can be determined. The Ct values of the candidate DNA aptamers are shown in Fig. 2. Among them, aptamer candidates SC2_R4_3 (10.71 ± 0.05), SC2_R4_4 (7.78 ± 0.04), and SC2_R4_5 (10.93 ± 0.09) exhibited the highest binding affinities. Notably, SC2_R4_4 displayed the highest binding affinity among the three aptamer candidates.

In addition, the SELEX method and qPCR were employed following the same protocol as in this study to compare the binding affinities of the DNA aptamers developed in other studies (Table 2). A comparison between the three candidate DNA aptamers identified in this study and four types of DNA aptamers from previous studies, showed that all candidate aptamers exhibited higher binding affinities (Fig. 3). These results indicate that the DNA aptamer developed in our study has a higher binding affinity to the SARS-CoV-2 spike protein.

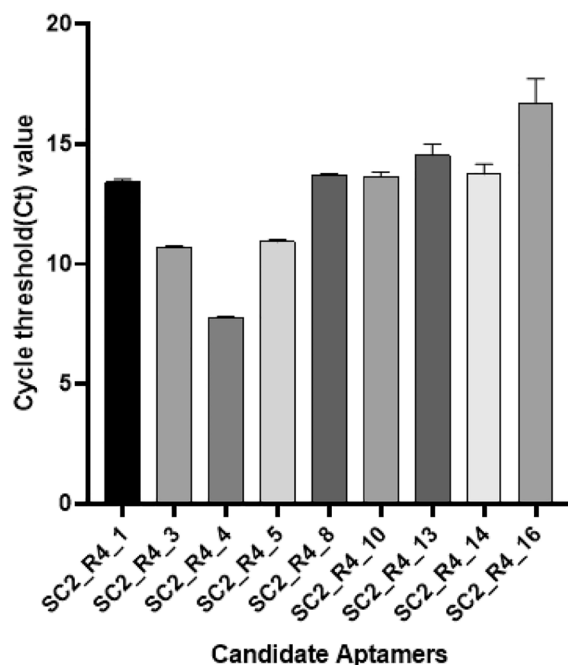


Figure 2. Comparison of cycle threshold (Ct) values between aptamers. The Y-axis represents the Ct values, and each bar on the X-axis corresponds to candidate DNA aptamer. The Ct value serves as an indicator of the DNA aptamer concentrations during the SELEX process under identical conditions. Error bars indicate the standard deviations obtained from three parallel tests.

No	Name	5'-Oligo Seq-3'	References
1	nCoV-S1-A1	AGC AGC ACA GAG GTC AGA TGC CGC AGG CAG CTG CCA TTA GTC TCT ATC CGT GAC GGT ATG CCT ATG CGT GCT ACC GTG AA	20
2	SP6	GGG AGA GGA GGG AGA TAG ATA TCA ACC CAT GGT AGG TAT TGC TTG GTA GGG ATA GTG GGC TTG ATG TTT CGT GGA TGC CAC AGG AC	45
3	CoV2-RBD-1	ATC CAG AGT GAC GCA GCA CCG ACC TTG TGC TTT GGG AGT GCT GGT CCA AGG GCG TTA ATG GAC ACG GTG GCT TAG T	44
4	CoV2-RBD-4	ATC CAG AGT GAC GCA GCA TTT CAT CGG GTC CAA AAG GGG CTG CTC GGG ATT GCG GAT ATG GAC ACG GTG GCT TAG T	44

Table 2. List of recently reported DNA aptamers.

Secondary structures of candidate DNA aptamers

The secondary structures of the three DNA aptamers with the highest binding affinities were predicted using the RNAfold web server based on the principle of minimum folding energy. The predicted secondary structures of these DNA aptamers displayed stable loop-stem and bulge structures. This suggests that the stem loop and bulge structures likely play significant roles in the binding of DNA aptamers to the SARS-CoV-2 spike protein. Figure 4 illustrates the predicted secondary structures of aptamers SC2_R4_3, SC2_R4_4, and SC2_R4_5, along with their respective minimum free energies (ΔG) of -14.86 , -11.78 , and -12.17 kcal/mol.

DNA aptamers suppress pro-inflammatory responses by interfering with the spike protein/ACE2 interaction

Numerous studies have demonstrated that proinflammatory cytokine levels increase during SARS-CoV-2 infection^{34–36}. It is also well-known that the interaction between the ACE2 receptor and the spike protein of SARS-CoV-2 leads to a pro-inflammatory response^{37–42}. Therefore, we aimed to confirm whether the developed DNA aptamer targeting the SARS-CoV-2 spike protein could reduce the pro-inflammatory response by interfering with the spike protein/hACE2 interaction. Consequently, we investigated the effect of the selected aptamer on pro-inflammatory signaling pathways.

To enhance the response to the SARS-CoV-2 spike protein, we overexpressed ACE2 in HEK293 cells. HEK293 cells were transiently transfected with the pcDNA3.1-E. V or pcDNA3.1-ACE2, and the overexpression of ACE2 was confirmed by RT-PCR and WB (Fig. 5a). Subsequently, ACE2-overexpressing HEK293 cells were treated with the selected DNA aptamers and SARS-CoV-2 spike proteins. As a result, we observed a decrease in the expression levels of pro-inflammatory cytokines Il-1 β , IL-6, and TNF- α upon treatment with all types of DNA aptamers (Fig. 5b–d). In addition, cytokine levels decreased with the DNA aptamers (Fig. 5e–g). The reduction

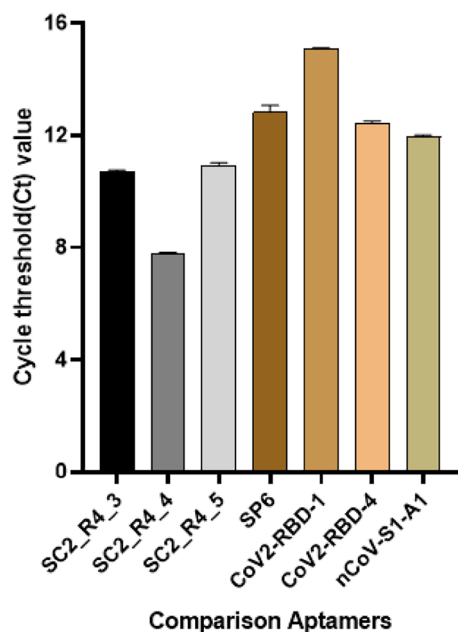


Figure 3. Comparison of binding affinity with other DNA aptamers. The Y-axis represents the Ct values, and each bar on the X-axis represents the comparison between the selected DNA aptamers and the comparative DNA aptamers. The experiment was conducted using the same method as before. Error bars indicate the standard deviation obtained from three parallel tests.

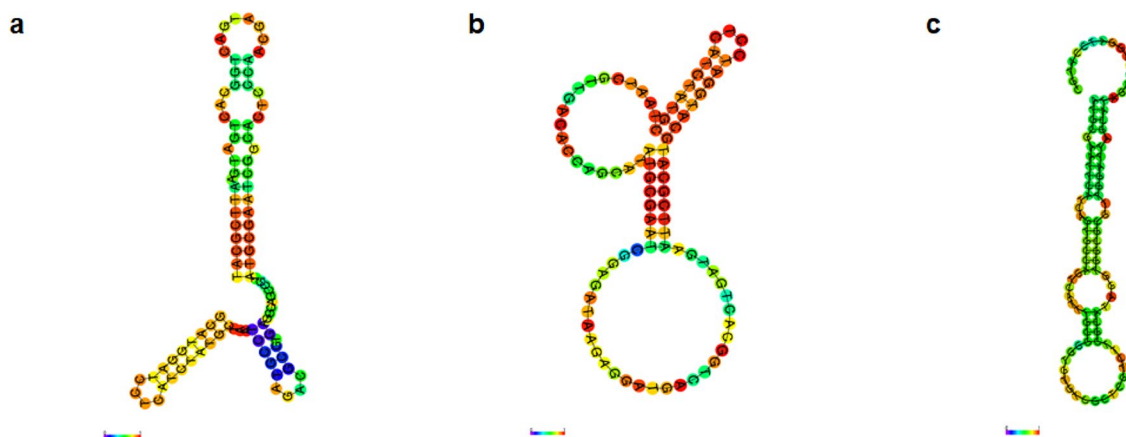


Figure 4. The minimum free energy (MFE) secondary structure of DNA aptamers predicted by the RNAfold web server. The structural predictions were generated using the RNAfold server from the Vienna websuit (<http://rna.tbi.univie.ac.at>). The predicted secondary structures of (a) SC2_R4_3, (b) SC2_R4_4, and (c) SC2_R4_5 exhibited stable loop-stem and bulge structures. The base pair probabilities calculated by the web server are color-coded, with blue representing the lowest probability (0) and red representing the highest probability (1).

in cytokine levels exhibited a similar pattern to that of the binding affinity of the DNA aptamers to the SARS-CoV-2 spike protein (Fig. 5b–g). These findings suggest that the developed DNA aptamer inhibits the interaction between the SARS-CoV-2 spike protein and ACE2 by binding to them.

Discussion

The SARS-CoV-2 spike protein on the viral envelope can bind to ACE2 via the RBD in the S1 subunit⁶. Compared to RNA aptamers, DNA aptamers are more stable and therefore easier to chemically modify and immobilize⁴³. In this study, nine candidate DNA aptamers that bind to the SARS-CoV-2 spike protein were developed using the SELEX method. The binding affinities of the selected DNA aptamers were compared with the Ct values obtained using qPCR. The best aptamers for SARS-CoV-2 spike protein binding identified in this study were SC2_R4_3, SC2_R4_4, and SC2_R4_5. In addition, the superiority of our aptamers was confirmed by comparing their binding affinities with those of aptamers developed in previous studies^{20,44,45}. These results showed that the

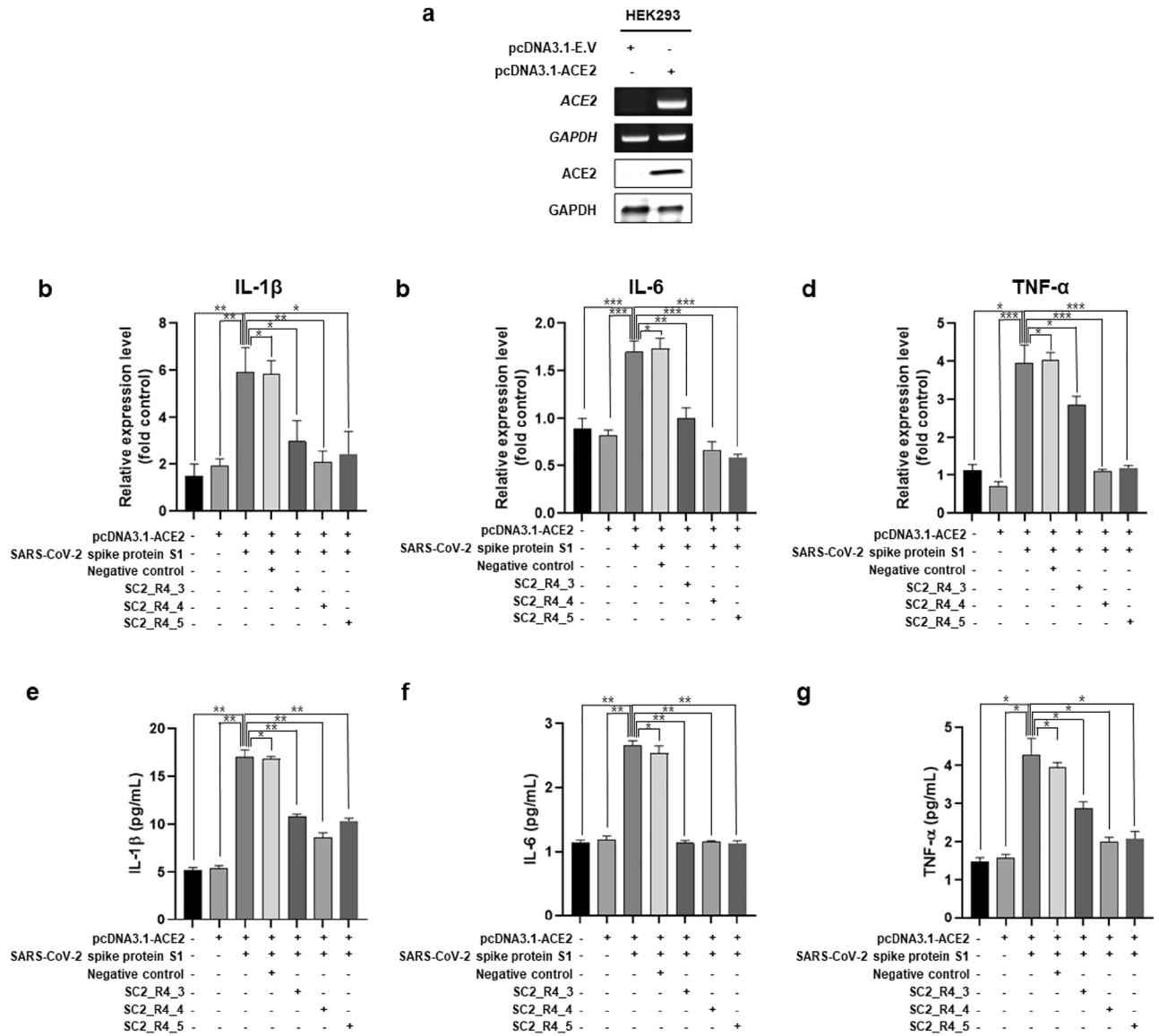


Figure 5. Inhibitory effect of DNA aptamers on the pro-inflammatory response induced by SARS-CoV-2 spike protein in HEK293 cells. **(a)** HEK293 cells were transfected with pcDNA3.1-E.V or pcDNA3.1-ACE2 over-expression levels were detected by RT-PCR and WB. GAPDH was used positive control. **(b–d)** To confirm the inhibition of the pro-inflammatory response of the candidate aptamer, 0.4 μ g/mL of SARS-CoV-2 spike protein was bound with 1 μ g/mL of DNA aptamers at 4 $^{\circ}$ C on a rotator for 30 min. The binders were then treated for 24 h in ACE2-overexpressing HEK293 cells. After incubation, mRNA expression of IL-1 β **(b)**, IL-6 **(c)**, and TNF- α **(d)** were confirmed using qPCR, and cytokine levels [IL-1 β **(e)**, IL-6 **(f)**, and TNF- α **(g)**] of culture medium was measured using ELISA kit. Negative control is random sequence ssDNA aptamer. The bar graph shows mRNA expression normalized to GAPDH **(b,c,d)** and cytokine concentration **(e,f,g)**. (*, **, ***, and ns indicate $P < 0.1$, $P < 0.01$, $P < 0.001$, and not significant, respectively).

affinity of our selected aptamer for the SARS-CoV-2 spike protein was higher than that of the other comparative DNA aptamers.

To gather structural information on candidate aptamers, their secondary structures were predicted by the RNAfold Webserver using DNA parameters²⁷. The predicted secondary structures of three selected aptamers are shown in Fig. 4. The minimum free energy (MFE) predicted the secondary structures of the aptamers, including loop-stem and bulge structures.

Finally, we investigated the effect of the selected aptamer on cellular responses through molecular experiments. Recent studies suggest that an excessive pro-inflammatory response in the host drives the disease severity and mortality in patients^{35,36}. In addition, the proinflammatory factors TNF- α , IL-1 β , and IL-6 have been suggested as biomarkers of SARS-CoV-2 infection³⁴. Thus, we confirmed that the developed DNA aptamers reduced the proinflammatory response by interfering with the spike protein/ACE2 interaction. These findings indicated that all types of DNA aptamers successfully decreased the levels of pro-inflammatory cytokines.

In this study, a DNA aptamer that binds to the SARS-CoV-2 spike protein was developed; however, direct binding between the aptamer and protein could not be confirmed. Since various studies have recently been conducted to measure the binding affinity of aptamers using qPCR^{30–33}, we were able to indirectly confirm the binding between the aptamer and protein by measuring the Ct value. In addition, indirect binding between the DNA aptamer and SARS-CoV-2 spike protein was confirmed by utilizing the pro-inflammatory response caused by surface interaction between the ACE2 receptor and SARS-CoV-2 spike protein^{37–42}. As expected, the decrease in cytokine levels showed a pattern similar to that of the binding affinity of DNA aptamers for the SARS-CoV-2 spike protein. As a result, we could not confirm the molecular mechanism by which SC2_R4_3, SC2_R4_4, and SC2_R4_5 inhibited viral infection, but we could indirectly confirm that the DNA aptamer interfered with the binding of the SARS-CoV-2 spike protein to ACE2.

In conclusion, we developed DNA aptamers that bind to the SARS-CoV-2 spike protein and have the potential to inhibit SARS-CoV-2 infection. The three selected DNA aptamers had higher affinities than DNA aptamers developed in other studies. Furthermore, we confirmed that the developed DNA aptamer reduced the pro-inflammatory response by interfering with the spike protein/ACE2 interaction. In conclusion, DNA aptamers can be used to inhibit SARS-CoV-2 infection, and this study intends to provide a direction for the development of new therapeutics.

Data availability

The datasets generated and/or analysed during the current study are not publicly available due the confidentiality reasons, but are available from the corresponding author on reasonable request.

Received: 10 January 2024; Accepted: 27 March 2024

Published online: 29 March 2024

References

- Gorbalenya, A. E. *et al.* The species severe acute respiratory syndrome-related coronavirus: classifying 2019-nCoV and naming it SARS-CoV-2. *Nat. Microbiol.* **5**, 536–544 (2020).
- Wrapp, D. *et al.* Cryo-EM structure of the 2019-nCoV spike in the prefusion conformation. *Science* **367**, 1260–1263 (2020).
- Hu, B., Guo, H., Zhou, P. & Shi, Z.-L. Characteristics of SARS-CoV-2 and COVID-19. *Nat. Rev. Microbiol.* **19**, 141–154 (2021).
- Jafarzadeh, A., Chauhan, P., Saha, B., Jafarzadeh, S. & Nemati, M. Contribution of monocytes and macrophages to the local tissue inflammation and cytokine storm in COVID-19: Lessons from SARS and MERS, and potential therapeutic interventions. *Life Sci.* **257**, 118102 (2020).
- Tang, Y. *et al.* Cytokine storm in COVID-19: The current evidence and treatment strategies. *Front. Immunol.* **11**, 1708 (2020).
- Hatmal, M. M. M. *et al.* Comprehensive structural and molecular comparison of spike proteins of SARS-CoV-2, SARS-CoV and MERS-CoV, and their interactions with ACE2. *Cells* **9**, 2638 (2020).
- Eftekhari, A. *et al.* A comprehensive review of detection methods for SARS-CoV-2. *Microorganisms* **9**, 232 (2021).
- Liu, R. *et al.* Positive rate of RT-PCR detection of SARS-CoV-2 infection in 4880 cases from one hospital in Wuhan, China, from Jan to Feb 2020. *Clin. Chim. Acta* **505**, 172–175 (2020).
- Bwire, G. M., Majigo, M. V., Njiro, B. J. & Mawazo, A. Detection profile of SARS-CoV-2 using RT-PCR in different types of clinical specimens: A systematic review and meta-analysis. *J. Med. Virol.* **93**, 719–725 (2021).
- Lassaunière, R. *et al.* Evaluation of nine commercial SARS-CoV-2 immunoassays. *MedRxiv* (2020).
- Wang, D. *et al.* Rapid lateral flow immunoassay for the fluorescence detection of SARS-CoV-2 RNA. *Nat. Biomed. Eng.* **4**, 1150–1158 (2020).
- Li, Z. *et al.* Development and clinical application of a rapid IgM-IgG combined antibody test for SARS-CoV-2 infection diagnosis. *J. Med. Virol.* **92**, 1518–1524 (2020).
- Polack, F. P. *et al.* Safety and efficacy of the BNT162b2 mRNA Covid-19 vaccine. *N. Engl. J. Med.* **383**, 2603–2615 (2020).
- Baden, L. R. *et al.* Efficacy and safety of the mRNA-1273 SARS-CoV-2 vaccine. *N. Engl. J. Med.* **384**, 403–416 (2021).
- Corbett, K. S. *et al.* SARS-CoV-2 mRNA vaccine design enabled by prototype pathogen preparedness. *Nature* **586**, 567–571 (2020).
- Cao, B. *et al.* A trial of lopinavir–ritonavir in adults hospitalized with severe Covid-19. *N. Engl. J. Med.* **382**, 1787–1799 (2020).
- Ju, B. *et al.* Human neutralizing antibodies elicited by SARS-CoV-2 infection. *Nature* **584**, 115–119 (2020).
- Wang, C. *et al.* A human monoclonal antibody blocking SARS-CoV-2 infection. *Nat. Commun.* **11**, 2251 (2020).
- Sun, M. *et al.* Aptamer blocking strategy inhibits SARS-CoV-2 virus infection. *Angew. Chem. Int. Ed.* **60**, 10266–10272 (2021).
- Yang, G. *et al.* Identification of SARS-CoV-2-against aptamer with high neutralization activity by blocking the RBD domain of spike protein 1. *Signal Transduct. Target. Ther.* **6**, 227 (2021).
- Liu, X. *et al.* Neutralizing aptamers block S/RBD-ACE2 interactions and prevent host cell infection. *Angew. Chem. Int. Ed.* **60**, 10273–10278 (2021).
- Ellington, A. D. & Szostak, J. W. In vitro selection of RNA molecules that bind specific ligands. *Nature* **346**, 818–822 (1990).
- Toh, S. Y., Citartan, M., Gopinath, S. C. & Tang, T.-H. Aptamers as a replacement for antibodies in enzyme-linked immunosorbent assay. *Biosens. Bioelectron.* **64**, 392–403 (2015).
- Tuerk, C. & Gold, L. Systematic evolution of ligands by exponential enrichment: RNA ligands to bacteriophage T4 DNA polymerase. *Science* **249**, 505–510 (1990).
- Thiel, K. W. & Giangrande, P. H. Therapeutic applications of DNA and RNA aptamers. *Oligonucleotides* **19**, 209–222 (2009).
- Navien, T. N., Thevendran, R., Hamdani, H. Y., Tang, T.-H. & Citartan, M. In silico molecular docking in DNA aptamer development. *Biochimie* **180**, 54–67 (2021).
- Gruber, A. R., Lorenz, R., Bernhart, S. H., Neuböck, R. & Hofacker, I. L. The vienna RNA websuite. *Nucleic Acids Res.* **36**, W70–W74 (2008).
- Bartolomé, A., Liang, J., Wang, P., Ho, D. D. & Pajvani, U. B. Angiotensin converting enzyme 2 is a novel target of the γ -secretase complex. *Sci. Rep.* **11**, 9803 (2021).
- Darmostuk, M., Rimpelova, S., Gbelcova, H. & Ruml, T. Current approaches in SELEX: An update to aptamer selection technology. *Biotechnol. Adv.* **33**, 1141–1161 (2015).
- Li, K. *et al.* Selection and preliminary application of a single stranded DNA aptamer targeting colorectal cancer serum. *RSC Adv.* **9**, 38867–38876 (2019).
- Avci-Adali, M. *et al.* Absolute quantification of cell-bound DNA aptamers during SELEX. *Nucleic Acid Ther.* **23**, 125–130 (2013).
- Amini, R. *et al.* Aptamers for SARS-CoV-2: Isolation, characterization, and diagnostic and therapeutic developments. *Anal. Sens.* **2**, e202200012 (2022).

33. Liu, R., He, L., Hu, Y., Luo, Z. & Zhang, J. A serological aptamer-assisted proximity ligation assay for COVID-19 diagnosis and seeking neutralizing aptamers. *Chem. Sci.* **11**, 12157–12164 (2020).
34. Tripathy, A. S. *et al.* Pro-inflammatory CXCL-10, TNF- α , IL-1 β , and IL-6: Biomarkers of SARS-CoV-2 infection. *Arch. Virol.* **166**, 3301–3310 (2021).
35. Mehta, P. *et al.* COVID-19: Consider cytokine storm syndromes and immunosuppression. *The Lancet* **395**, 1033–1034 (2020).
36. Merad, M. & Martin, J. C. Pathological inflammation in patients with COVID-19: a key role for monocytes and macrophages. *Nat. Rev. Immunol.* **20**, 355–362 (2020).
37. Singh, R. D. *et al.* The spike protein of SARS-CoV-2 induces heme oxygenase-1: Pathophysiologic implications. *Biochim. Biophys. Acta* **1868**, 166322 (2022).
38. Lee, A. R. *et al.* SARS-CoV-2 spike protein promotes inflammatory cytokine activation and aggravates rheumatoid arthritis. *Cell Commun. Signal.* **21**, 44 (2023).
39. Rather, I. A. *et al.* The inhibition of SARS-CoV-2 and the modulation of inflammatory responses by the probio65 extract of *Lactobacillus sakei*. *Vaccines* **10**, 2106 (2022).
40. Alzahrani, O. R., Hawsawi, Y. M., Alanazi, A. D., Alatwi, H. E. & Rather, I. A. In vitro evaluation of *Leuconostoc mesenteroides* cell-free-supernatant GBUT-21 against SARS-CoV-2. *Vaccines* **10**, 1581 (2022).
41. Tran, H. T. T., Le, N. P. K., Gigl, M., Dawid, C. & Lamy, E. Common dandelion (*Taraxacum officinale*) efficiently blocks the interaction between ACE2 cell surface receptor and SARS-CoV-2 spike protein D614, mutants D614G, N501Y, K417N and E484K in vitro. *BioRxiv* **74**, e13525 (2021).
42. Rather, I. A. *et al.* Potential adjuvant therapeutic effect of *Lactobacillus plantarum* probio-88 postbiotics against SARS-CoV-2. *Vaccines* **9**, 1067 (2021).
43. Song, K.-M., Lee, S. & Ban, C. Aptamers and their biological applications. *Sensors* **12**, 612–631 (2012).
44. Song, Y. *et al.* Discovery of aptamers targeting the receptor-binding domain of the SARS-CoV-2 spike glycoprotein. *Anal. Chem.* **92**, 9895–9900 (2020).
45. Schmitz, A. *et al.* A SARS-CoV-2 spike binding DNA Aptamer that inhibits Pseudovirus infection by an RBD-independent mechanism. *Angew. Chem. Int. Ed.* **60**, 10279–10285 (2021).

Author contributions

Conceptualization, W.K., J.H.C. and S.-J.K.; methodology, W.K., E.S.S., S.H.L., S.H.Y., and S.-J.K.; formal analysis, W.K., E.S.S., and S.H.L.; investigation, W.K., E.S.S., and S.H.L.; writing—original draft, W.K., S.H.Y., and S.-J.K.; Writing—review and editing, W.K., S.H.Y., J.H.C. and S.-J.K.; funding acquisition, W.K., S.H.Y., and S.-J.K. All authors have read and agreed to the published version of the manuscript.

Funding

This work was supported by the Technology Development Program (S3046049) funded by the Ministry of SMEs and Startups (MSS, Korea), and a National Research Foundation of Korea (NRF) grant funded by the Korean Government (MSIT) (No. RS-2023-00244707 and 2021R1A6A3A01086424), and the Learning & Academic Research Institution for Master's Ph.D. students, and Postdocs (LAMP) program (No. RS-2023-00285353).

Competing interests

Authors E.S.S., S.H.L., and S.H.Y. employed the UNICOMPANY software. The authors declare that this study was conducted in the absence of commercial or financial relationships that could be construed as potential conflicts of interest.

Additional information

Supplementary Information The online version contains supplementary material available at <https://doi.org/10.1038/s41598-024-58315-0>.

Correspondence and requests for materials should be addressed to S.-J.K.

Reprints and permissions information is available at www.nature.com/reprints.

Publisher's note Springer Nature remains neutral with regard to jurisdictional claims in published maps and institutional affiliations.



Open Access This article is licensed under a Creative Commons Attribution 4.0 International License, which permits use, sharing, adaptation, distribution and reproduction in any medium or format, as long as you give appropriate credit to the original author(s) and the source, provide a link to the Creative Commons licence, and indicate if changes were made. The images or other third party material in this article are included in the article's Creative Commons licence, unless indicated otherwise in a credit line to the material. If material is not included in the article's Creative Commons licence and your intended use is not permitted by statutory regulation or exceeds the permitted use, you will need to obtain permission directly from the copyright holder. To view a copy of this licence, visit <http://creativecommons.org/licenses/by/4.0/>.

© The Author(s) 2024